

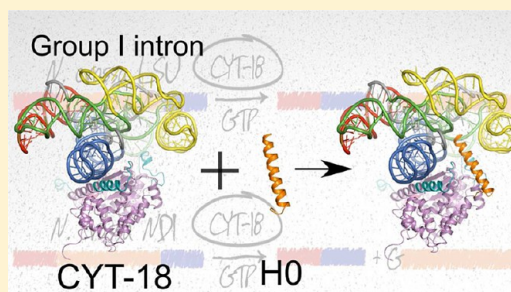
An in Vitro Peptide Complementation Assay for CYT-18-Dependent Group I Intron Splicing Reveals a New Role for the N-Terminus

Chun Geng and Paul J. Paukstelis*

University of Maryland, Department of Chemistry and Biochemistry, Center for Biomolecular Structure and Organization, College Park, Maryland 20742, United States

Supporting Information

ABSTRACT: The mitochondrial tyrosyl tRNA synthetase from *Neurospora crassa* (CYT-18 protein) is a bifunctional group I intron splicing cofactor. CYT-18 is capable of splicing multiple group I introns from a wide variety of sources by stabilizing the catalytically active intron structures. CYT-18 and mt TyrRSs from related fungal species have evolved to assist in group I intron splicing in part by the accumulation of three N-terminal domain insertions. Biochemical and structural analysis indicate that the N-terminal insertions serve primarily to create a structure-stabilizing scaffold for critical tertiary interactions between the two major RNA domains of group I introns. Previous studies concluded that the primarily α -helical N-terminal insertion, H0, contributes to protein stability and is necessary for splicing the *N. crassa* ND1 intron but is dispensable for splicing the *N. crassa* mitochondrial LSU intron. Here, we show that CYT-18 with a complete H0 deletion retains residual ND1 intron splicing activity and that addition of the missing N-terminus *in trans* is capable of restoring a significant portion of its splicing activity. The development of this peptide complementation assay has allowed us to explore important characteristics of the CYT-18/group I intron interaction including the stoichiometry of H0 in intron splicing and the importance of specific H0 residues. Evaluation of truncated H0 peptides in this assay and a re-examination of the CYT-18 crystal structure suggest a previously unknown structural role of the first five N-terminal residues of CYT-18. These residues interact directly with another splicing insertion, making H0 a central structural element responsible for connecting all three N-terminal splicing insertions.



The *Neurospora crassa* mitochondrial tyrosyl-tRNA synthetase (mt TyrRS; CYT-18 protein) and the mt TyrRSs from other Pezizomycotina fungi are multifunctional proteins responsible for aminoacylating mt tRNA^{Tyr} and promoting mt group I intron splicing.^{1,2} Previous studies showed that CYT-18 recognizes conserved structural features of the group I intron catalytic core and promotes splicing by stabilizing the catalytically active RNA structure.^{3–5} Chemical structure modification analysis showed that CYT-18 does not recognize introns in a sequence-specific manner but instead recognizes the three-dimensional structure of the phosphodiester backbone.^{5,6} Though group I intron primary sequences can vary greatly, their conserved three-dimensional structures allow CYT-18 to recognize and promote splicing of diverse group I introns.^{3,7–9} Biochemical and genetic experiments led to a model that CYT-18 functions in splicing by first interacting with the intron P4–P6 domain, followed by contacts with the P3–P9 domain that stabilizes the two extended RNA domains in the correct orientation relative to non-native structures to generate a catalytically active intron conformation.^{3–5,7,10}

Bacterial and mt TyrRSs are both comprised of an N-terminal catalytic domain, an intermediate α -helical domain, and a C-terminal tRNA-binding domain. Despite significant structural homology between bacterial and mt TyrRSs, group I intron splicing activity has only been demonstrated for mt TyrRSs of fungi belonging to the subphylum Pezizomycotina.²

The Pezizomycotina mt TyrRSs are distinguished by a number of positionally conserved insertions, including an N-terminal extension (H0), two small insertions in the catalytic domain (Ins1 and Ins2), and three insertions in the C-terminal domain (Ins3, 4, and 5).^{2,11}

The N-terminal domain insertion with the highest sequence conservation among the Pezizomycotina mt TyrRSs and most thoroughly studied biochemically is the N-terminal extension, H0.^{2,12} H0 (residues 33–61) is primarily an amphipathic α -helix (residues 39–60) that represents the first regular secondary structure element of CYT-18 following cleavage of the mt targeting peptide. Biochemical studies demonstrated that H0 was important for intron splicing but dispensable for TyrRS activities. Significantly, all previous CYT-18 N-terminal truncations tested began after Phe37. Deletion of as few as four residues (Δ 38–41) abolished splicing activity;¹¹ however, an even more extensive deletion that included the entire H0 α -helix (Δ 38–59) retained splicing activity for the mt LSU intron but was unable to splice the *N. crassa* ND1 intron.¹² Conversely, CYT-18's C-terminal domain was required for splicing the *N. crassa* mt LSU intron but was dispensable for

Received: December 3, 2013

Revised: January 21, 2014

Published: February 12, 2014



splicing the ND1 intron. This differential dependence on these structural elements suggested that CYT-18 utilizes different regions to compensate for different RNA structural defects in non-self-splicing group I introns.¹²

Structural studies of CYT-18 provided significant clues for the structural and functional role of H0 in group I intron splicing. The crystal structure of C-terminally truncated CYT-18 (CYT-18/ Δ 424–669) showed H0 connected to the highly conserved TyrRS core through Gly62 and that it is stabilized against the protein core by primarily localized hydrophobic interactions through H0 residues Trp52, Arg55, and Ile59.¹³ This analysis was consistent with both genetic experiments that identified these residues as among the most highly conserved in splicing-competent proteins from H0 mutant libraries¹² and in amino acid conservation in *Pezizomycotina* mt TyrRSs.² The seven N-terminal-most residues of H0 (including the initiating Met that would not be present in the mature mt protein) were not built in this crystal structure, due to weak electron density as well as ambiguity resulting from the proximity of these N-terminal residues and flexible C-terminal residues from a symmetry-related monomer.¹³

A co-crystal structure of a splicing active C-terminally truncated CYT-18 protein (CYT-18/ Δ 424–669) with a group I intron RNA (the bacteriophage Twort *orf*142-I2 ribozyme) revealed key features of the RNA–protein interface and showed that H0, Ins1, and Ins2 from one subunit of the homodimer interact directly with the group I intron catalytic core and stabilize and/or promote key tertiary interactions.¹⁴ H0 and Ins1 interact with one another through side chain contacts to form a scaffold for group I intron binding at the junction of the two RNA domains, while Ins2 interacts in the minor groove of the intron's P9 helix. On the basis of the co-crystal structure, H0 from one subunit of the CYT-18 dimer helps to establish the correct orientations of the P4–P6 and P3–P9 domains through interactions with the J3/4, J6/7 junctions and P7. H0 from the other subunit of the CYT-18 dimer was in proximity to P5 of the intron RNA, but its role, if any, in splicing was not clear. Despite being determined at low-resolution, this co-crystal structure showed contiguous backbone electron density for the previously unobserved N-terminal H0 residues.

In this study, we explore the role of H0 in group I intron splicing through development of an *in vitro* peptide complementation splicing assay. We have examined the first complete CYT-18 H0 deletion (CYT-18/ Δ 33–61) and found it retains residual splicing activity. Significantly, we show that CYT-18/ Δ 33–61 splicing activity is greatly restored through the addition of the N-terminal H0 peptide *in trans*. Titration experiments coupled with burst kinetic analysis indicates that H0 bound to one subunit of the CYT-18 dimer is sufficient to promote intron splicing. Failure of short N-terminally truncated H0 peptides to restore splicing in this assay and the inability of a CYT-18 mutant lacking just the first five H0 residues to promote splicing indicate a previously unrecognized role for the N-terminal-most residues of CYT-18. Reanalysis of the CYT-18/ Δ 424–669 crystal structure indicates that these N-terminal residues interact directly with Ins2, providing a new role for H0 as a structural link connecting all three N-terminal splicing insertions.

■ EXPERIMENTAL PROCEDURES

Protein Expression and Purification. CYT-18 protein was expressed and purified as previously described.¹³ The CYT-18/ Δ 33–61 and CYT-18/ Δ 33–37 open reading frames, both with

an N-terminal hexahistidine tag followed by a tobacco etch virus (TEV) protease recognition sequence, were cloned into expression vector pET-11d (Novagen) and confirmed by sequencing. Proteins were expressed by autoinduction¹⁵ in *Escherichia coli* HMS174(DE3) and purified by sequential Ni²⁺ columns as previously described for the *Aspergillus nidulans* mt TyrRS.² All proteins were dialyzed against 25 mM Tris-HCl (pH 7.5), 500 mM KCl, and 50% (v/v) glycerol, flash frozen, and stored at –80 °C.

Denaturation and Renaturation. Protein denaturation was done by mixing 200 μ L of 100 μ M CYT-18 dimer with 1.8 mL of denaturation buffer containing 25 mM Tris-HCl (pH 7.5), 500 mM KCl, 2 mM DTT, and 8 M urea and incubated for 10 min. Protein renaturation was done by buffer exchange using an Amicon Ultra 10K MWCO centrifugal filter concentrator. Urea was gradually removed by four cycles of centrifugation. A total of 4.5 mL of renaturation buffer containing 25 mM Tris-HCl (pH 7.5) and 500 mM KCl was added to the concentrator following concentration to 250 μ L. The final protein concentrations were determined by UV absorbance at 280 nm and adjusted to 500 nM for tyrosyl-adenylation assays (ϵ_{280} for CYT-18, CYT-18/ Δ 33–61 and CYT-18/ Δ 33–37 are respectively 96 680 M^{–1} cm^{–1}, 89 710 M^{–1} cm^{–1}, and 96 680 M^{–1} cm^{–1}). All steps were performed at 25 °C.

■ Peptide Synthesis, Expression, and Purification.

Except where noted, peptides utilized in the complementation assays were chemically synthesized and HPLC-purified (United Biosystems, Herndon, VA and NEO Biolab, Cambridge, MA). These peptides were directly dissolved in 10 mM Tris-HCl (pH 7.5), 10 mM KCl, and 50% (v/v) glycerol and stored at –80 °C. Several assays were performed with recombinant H0-WT peptide. The H0-WT peptide was cloned into vector pMAL-C2T, expressed via autoinduction in *E. coli* HMS174-(DE3) as a maltose-binding protein fusion that was cleavable by TEV protease. The fusion protein was purified by amylose affinity chromatography and cleaved, and the products were separated by size-exclusion chromatography. Both synthetic and recombinant peptides were verified by mass spectrometry. Concentrations were determined by UV absorbance at 280 nm (ϵ_{280} for H0-WT, H0-37, H0-42, and H0-46 are respectively 6970 M^{–1} cm^{–1}, 6970 M^{–1} cm^{–1}, 5690 M^{–1} cm^{–1}, and 5690 M^{–1} cm^{–1}).

Tyrosyl-Adenylation. Tyrosyl-adenylation assays were done in 25 μ L of reaction containing 500 nM protein, 5 mM ATP, 100 mM KCl, 10 mM MgCl₂, 144 mM Tris-HCl (pH 7.5), 0.1 unit of pyrophosphatase, and 5 μ Ci of L-[3,5-³H]-tyrosine (42.6 Ci mmol^{–1}; Perkin-Elmer). The reaction was initiated by addition of protein and incubated for 10 min at 30 °C. The samples were then filtered through nitrocellulose membrane (0.2 μ m pore size) to retain protein-bound tyrosyl-adenylate. Membranes were counted with a Beckman Coulter model LS6500 scintillation counter with ScintiVerse I scintillation cocktail (Fisher Scientific).

Group I Intron Splicing. ³²P-labeled RNA substrates were synthesized and prepared as described.² Splicing assays were done by adding CYT-18 protein to intron RNA to a final reaction volume of 25 μ L containing 5 mM MgCl₂, 25 mM Tris-HCl (pH 7.5), 1 mM DTT, 10% glycerol, 1 mM GTP-Mg²⁺, and indicated amounts of KCl at the specified temperatures. Splicing products were analyzed in either a 4% or 6% denaturing polyacrylamide gel that was dried and quantified with a Storm PhosphorImager (GE Bioscience). For peptide complementation experiments, indicated amounts of H0-WT or truncated H0 peptides were incubated with the

CYT-18/ Δ 33–61 protein at 25 °C for 1 h prior to being added to the splicing reaction. Burst kinetic analyses were done by incubating indicated amounts of the CYT-18 protein with a 2-fold excess of 32 P-labeled RNA substrates in the described splicing conditions lacking GTP-Mg $^{2+}$. These reactions were initiated by addition of 1 mM GTP-Mg $^{2+}$.

Crystal Structure Re-Evaluation. Structure factors and coordinates of the original CYT-18/ Δ 424–669 structure (PDBID: 1Y42) were downloaded from the Protein Data Bank.¹⁶ The missing N-terminal residues were built using Coot.¹⁷ The structure was refined using Refmac5¹⁸ using individual B-factor refinement, rather than the anisotropic B-factors as originally deposited.¹³ Structure figures were generated with PyMol.

RESULTS

Functional Assays and Stability of CYT-18/ Δ 33–61 Protein. To further examine the role of the CYT-18-specific H0 insertion, we constructed the first mutant with a complete H0 deletion (Figure 1). The CYT-18/ Δ 33–61 construct was

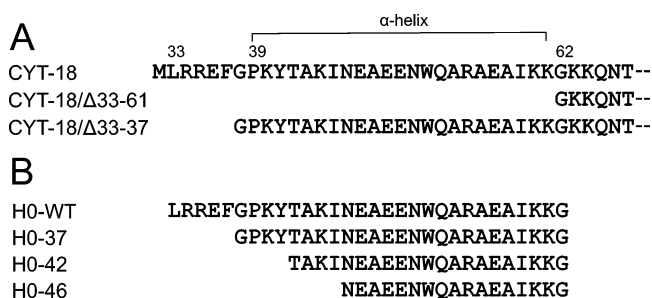


Figure 1. CYT-18 protein and peptide sequences. (A) The N-terminus of the mature CYT-18 proteins used in this study. Residues 1–32 of CYT-18 are the mt localization peptide and are cleaved upon entry into the mt matrix. Met32 in the WT CYT-18 construct is present as a result of translation initiation of this construct. Residues 33–61 comprise the H0 N-terminal extension. The α -helical portion of H0 is denoted. (B) H0-derived peptides used in this study.

generated through addition of an N-terminal hexahistidine tag followed by a protease cleavage site (Materials and Methods). Immobilized metal affinity purification steps before and after removal of the 6XHis tag with TEV protease yielded >95% pure protein (judged by Coomassie stained SDS-PAGE gels) with native Gly62 as the N-terminal most residue. This tandem purification approach allowed us to maintain high monovalent salt and glycerol concentrations throughout purification which was necessary to help maintain protein solubility.

Tyrosyl-Adenylation Activity and Protein Stability. We utilized tyrosyl adenylation assays to assess the activity of CYT-18/ Δ 33–61. Comparison of tyrosyl adenylation activity between A_{280} normalized wild-type (WT) CYT-18 and CYT-18/ Δ 33–61 showed little or no reduction in activity immediately after purification (Figure S1, Supporting Information). However, both previous studies¹² and our own observations indicated that N-terminally truncated CYT-18 was less stable than the WT protein, presumably due to solvent exposure of the hydrophobic H0 binding site on the core of the protein. We chose to assess the overall stability of the WT and truncated proteins by comparing their behavior to urea denaturation/renaturation (Figure S1A, Supporting Information). For WT CYT-18, we recovered ~50% of the input protein based on UV

absorbance following renaturation, with the final tyrosyl-adenylation activity nearly identical to that of the nondenatured sample. For CYT-18/ Δ 33–61, only ~15% of the total input protein was recovered and had only 13% of WT activity. The significant difference in both recovery and activity suggests that H0 plays an important role in maintaining an active protein conformation.

Group I Intron Splicing. Because of the lower stability of CYT-18/ Δ 33–61, we chose to examine its ability to splice group I introns at several temperatures. Consistent with previous results for other N-terminally truncated CYT-18 proteins, there was virtually no detectable specific ND1 intron splicing at 37 °C after 60 min (Figure 2A). Interestingly, ND1 splicing was readily detectable at 25° and 30 °C, though significantly decreased from the WT CYT-18 at these temperatures. One major lower molecular weight RNA product was observed only in the presence of the truncated protein and was more prominent with increased temperature. This aberrant product was discrete and observed from multiple protein preparations but was not dependent on the addition of exogenous guanosine (data not shown). This suggests it may be the result of a specific interaction formed readily in the absence of H0 that facilitates phosphodiester backbone cleavage. Previous assays demonstrated that N-terminally truncated CYT-18 was capable of splicing the *N. crassa* mt LSU intron.¹² Consistent with these findings, CYT-18/ Δ 33–61 spliced the mt LSU intron at both 25 and 30 °C, though with reduced activity compared to WT CYT-18 (Figure 2B). Similar to the previous study, CYT-18/ Δ 33–61 showed detectable but significantly decreased splicing activity at 37 °C. This had been previously attributed to decreased protein stability for the N-terminal truncation and was consistent with our stability results. At all temperatures, there is a greater accumulation of mt LSU intermediate splicing products for both WT and the truncated CYT-18 in comparison to previous studies. This is likely due to the less stringent monovalent salt concentration (50 vs 100 mM) in the experiments performed here.

Peptide Complementation by H0-WT. To quickly examine how different H0 mutants might affect group I intron splicing, we developed a peptide complementation assay. The full-length H0 peptide (H0-WT), or derivatives, were incubated with CYT-18/ Δ 33–61, and the reconstituted protein was tested for intron splicing at various concentrations, temperatures, and monovalent salt concentrations.

Temperature and Salt Dependence. Figure 3 shows CYT-18/ Δ 33–61's ability to splice the ND1 intron in the presence of 2-fold molar excess H0-WT peptide (with respect to the protein monomer), at three different temperatures and monovalent salt concentrations. The addition of the peptide enhanced the splicing activity of the CYT-18/ Δ 33–61 at all temperatures, with the greatest enhancement at 30 °C and at the two lowest salt concentrations. At 25 and 30 °C, the peptide complementation assay showed maximal activity at 50 mM KCl, while maximum splicing stimulation was observed at 25 mM KCl at 37 °C. For all temperatures tested, the amount of aberrant product was reduced in the presence of the peptide, though it was present to a greater extent at both elevated salt and temperatures. The reconstituted protein did not enhance splicing of the mtLSU intron (Figure S2, Supporting Information).

Concentration Dependence. Previous studies indicated marked protein concentration dependence for CYT-18 intron splicing when N- and C-terminal truncations were used.¹²

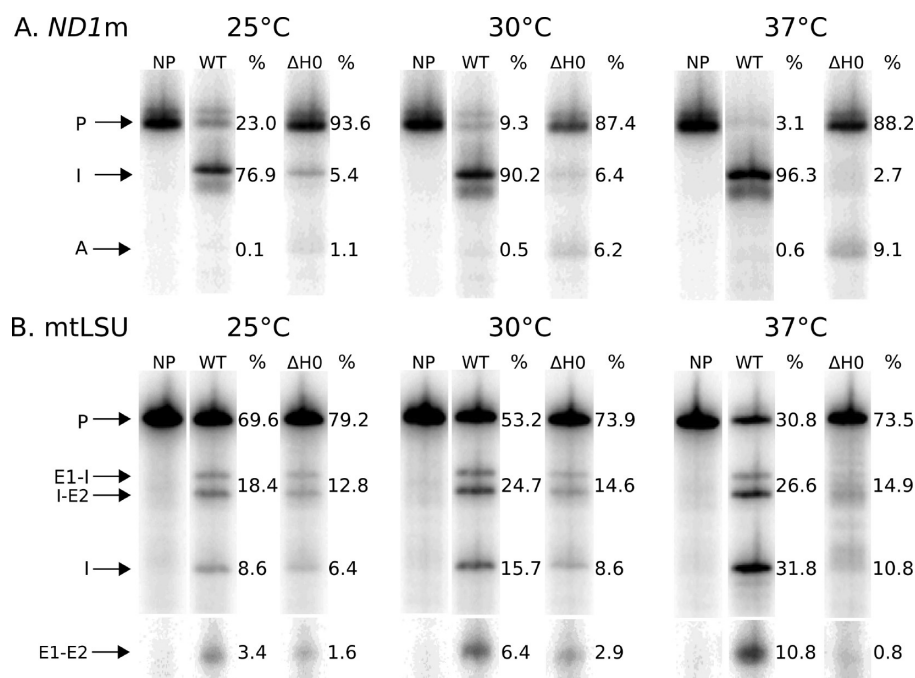


Figure 2. Comparison of CYT-18 and CYT-18/Δ33–61 group I intron splicing activity. Splicing was performed at 50 mM KCl at three temperatures for two *N. crassa* group I introns: (A) the ND1 intron and (B) the mt LSU intron. Products shown are following 60 min incubation at the given temperature. Final precursor RNA and protein dimer concentrations were 200 nM and 800 nM, respectively. A sample without protein (NP) is shown for each temperature. Percentages of the final RNA products are shown to the right of each product. Splicing intermediates were quantified as a single band. P, Precursor RNA; I, spliced intron; E1-I, 5' exon-intron; I-E2, intron-3' exon intermediate; E1-E2, ligated exons; A, aberrant RNA product. The 14 nt ligated exon product of ND1 splicing is not shown.

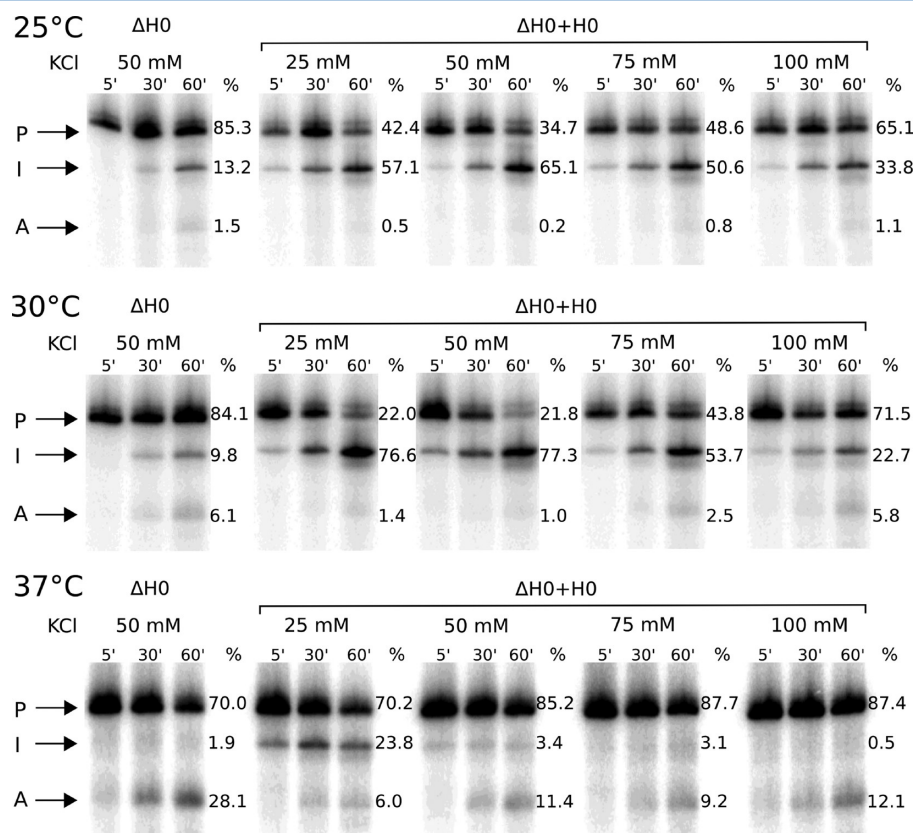


Figure 3. Peptide complementation by H0-WT. 200 nM ND1 intron was incubated under splicing conditions with 800 nM CYT-18/Δ33–61 (ΔH0) dimer alone or reconstituted with 3200 nM H0-WT peptide (ΔH0 + H0). Splicing with the reconstituted protein was performed at the three temperatures and four monovalent salt concentrations indicated. Three time points (5', 30', 60') are shown for each sample. Percentages of RNA products at 60' are shown to the right of each sample. P, Precursor RNA; I, spliced intron; A, aberrant RNA product.

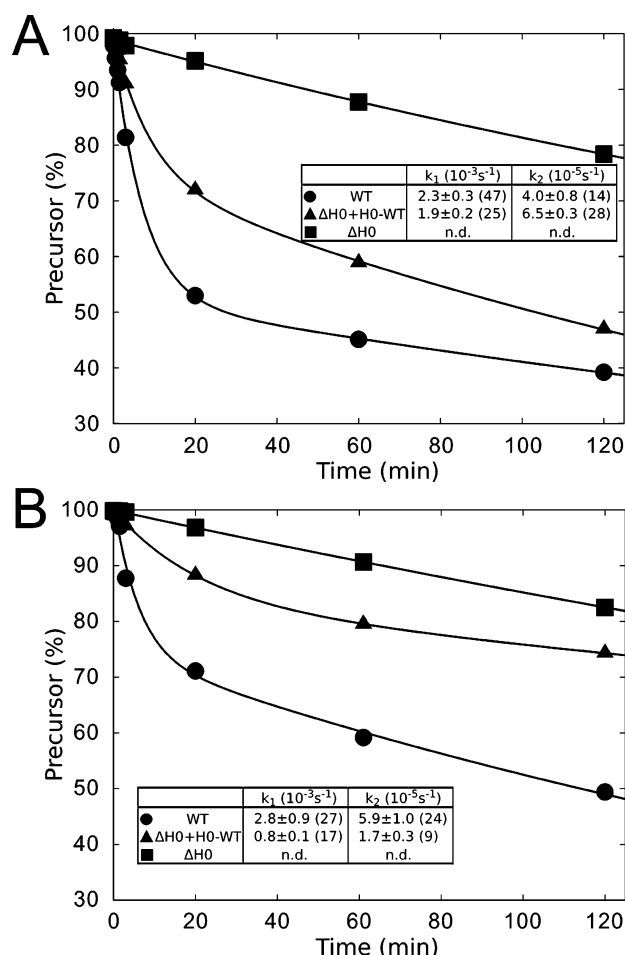


Figure 4. Concentration dependence of CYT-18/ Δ 33–61 complementation. Burst splicing reactions with precursor RNA in 2-fold molar excess to protein dimer were carried out at (A) 500 nM protein dimer and (B) 25 nM protein dimer. H0-WT peptide was maintained at a 2-fold molar excess to the CYT-18/ Δ 33–61 (Δ H0) dimer concentration. H0-WT used in these experiments was produced recombinantly (see Materials & Methods). k_{obs} for the two phases of splicing are shown with the amount of spliced product in each phase shown in parentheses.

To examine if this was also true with CYT-18/ Δ 33–61, we performed ND1 burst splicing at two different protein concentrations with RNA substrate in excess at 25 °C. The results are shown in Figure 4. CYT-18/ Δ 33–61 splicing in the absence of the H0-WT peptide was virtually identical at both the high and low protein concentrations with the precursor RNA disappearing linearly with time. Both WT CYT-18 and the reconstituted protein showed biphasic disappearance of RNA precursor, with a greater extent of splicing in the initial phase at the higher protein concentration. At the lower protein concentration, the WT CYT-18 initial rate was 3.5-fold faster than the reconstituted protein (2.8 vs $0.8 \times 10^{-3} \text{ s}^{-1}$), but these rates were comparable (2.3 vs $1.9 \times 10^{-3} \text{ s}^{-1}$) at the high protein concentration, indicating that the reconstituted protein at this concentration was nearly as active as WT. This suggests that the reconstituted protein is functionally equivalent to WT CYT-18 for splicing the ND1 intron. Because the peptide/dimer ratio was maintained at 2:1, the decreased splicing at the lower protein concentration could also reflect subsaturating conditions for H0-WT binding.

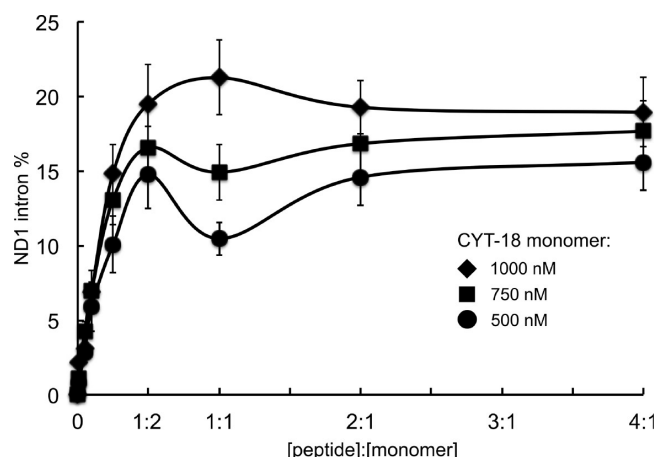


Figure 5. H0 stoichiometry. The indicated concentrations of CYT-18/ Δ 33–61 monomer were titrated with increasing concentration of H0-WT peptide prior to initiating the burst splicing reaction with precursor RNA in 2-fold molar excess to protein dimer. The percent intron product was determined at the 10 min time point and plotted against the molar ratio of peptide to CYT-18/ Δ 33–61 monomer. Points are the mean from three independent experiments. Error bars are standard deviations.

H0 Stoichiometry. The CYT-18/intron co-crystal structure suggested that the N-terminal insertions from just one of the dimer subunits was responsible for a majority of the intron contacts, with H0 from the other subunit in proximity to the intron's P5 loop. Using the H0 peptide complementation assay and burst kinetic analysis, we explored the necessary stoichiometry of H0 for intron splicing. Using multiple CYT-18 protein concentrations (500, 750, and 1000 nM CYT-18 monomer), we examined the ability of the H0-WT peptide to stimulate CYT-18/ Δ 33–61 splicing at ratios from 1:50 to 4:1 peptide/protein monomer. Figure 5 shows the percent spliced ND1 intron (relative to all RNA bands) versus the ratio of peptide to protein monomer after 10 min, a time point determined to be within the initial burst phase for the reconstituted protein. At all protein concentrations, the appearance of intron increased with the addition of peptide until reaching a peak at a peptide/monomer ratio of 1:2. Surprisingly, for 500 and 750 nM protein monomer, we observed a drop in the appearance of intron RNA at the 1:1 ratio. This decrease was not readily explainable but was observed in multiple independent experiments. In contrast, at 1000 nM CYT-18, there was a slight increase at the 1:1 ratio, though this was within error of measurements taken at 1:2 and 2:1. At all protein concentrations, the plateau was re-established at ratios of 2:1 or higher. These results indicate that single H0-WT peptide is sufficient to activate the CYT-18/ Δ 33–61 dimer.

The Five N-Terminal H0 Residues Are Required for Efficient Intron Splicing. We developed the H0 peptide complementation assay to provide a rapid way of exploring how modified H0 peptides can impact group I intron splicing. To begin, we examined a series of N-terminally truncated H0 peptides. Three different H0 peptides (H0-37, H0-42, and H0-46; Figure 1B) were tested. H0-WT and all three truncated peptides had similar spectra in circular dichroism measurements (Figure S3, Supporting Information), indicating that there were no major structural differences in solution. Surprisingly, when used in the peptide complementation assay, we found that none of the truncated peptides were capable of significantly

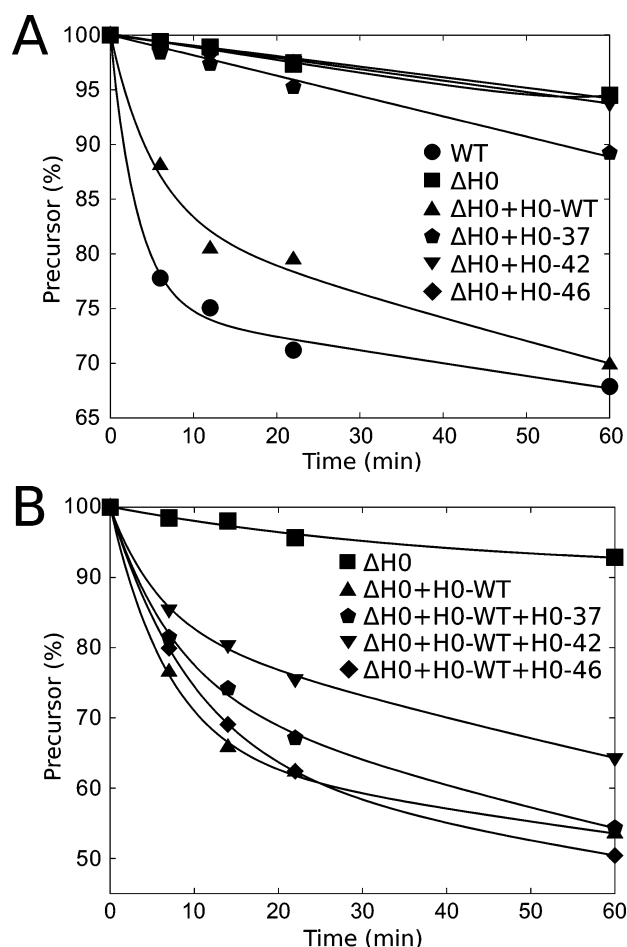


Figure 6. Peptide complementation with truncated H0 peptides. (A) Burst splicing time courses using 500 nM dimeric CYT-18 (WT), CYT-18/ Δ 33–61 (Δ H0) alone, and with equimolar H0 peptides to protein monomer. (B) Truncated peptide competition experiments. 500 nM CYT-18/ Δ 33–61 dimer was incubated with peptide mixtures containing 1 μ M H0-WT and 3 μ M N-terminally truncated H0 peptide. H0-WT used in these experiments was produced recombinantly (see Materials and Methods).

stimulating CYT-18/ Δ 33–61's ND1 intron splicing activity (Figure 6A). The lack of splicing could be the result of the peptides not binding to the truncated protein or their inability to productively contact the intron RNA when bound to CYT-18/ Δ 33–61. Competition assays using 3-fold molar excess of the truncated peptides to H0-WT revealed little (H0-42) or no (H0-37, H0-46) reduction in H0-WT's ability to activate CYT-18/ Δ 33–61's splicing activity (Figure 6B).

The inability for even the shortest N-terminal peptide truncations to bind or stimulate splicing in the peptide complementation assays indicated for the first time that these residues might have an important functional role in intron splicing. To compare how short N-terminal truncation might differ between the peptide complementation experiments and a truncated recombinant CYT-18, we created CYT-18/ Δ 33–37 protein which lacks just the first five amino acids. This protein did not have the stability issues observed with CYT-18/ Δ 33–61 and behaved identically to WT CYT-18 in tyrosyl-adenylation assays (Figure S1B, Supporting Information). However, consistent with observations from the peptide complementation assays, this N-terminally truncated protein had significantly reduced splicing activity for the ND1 intron

at 50 mM KCl at all three temperatures tested (Figure 7A). The aberrant splicing product was also present at levels comparable to CYT-18/ Δ 32–61 at 37 °C. Interestingly, the CYT-18/ Δ 33–37 also showed reduced splicing activity for the mt LSU intron when compared to WT CYT-18 (Figure 7B). Together, these results indicate that the N-terminal most residues of CYT-18 play a role in splicing both the ND1 and mt LSU introns.

Crystal Structure Re-Evaluation. The importance of H0's five N-terminal most residues for ND1 splicing in the context of both the full-length protein and the peptide complementation splicing led us to re-examine the CYT-18/ Δ 424–669 crystal structure for structural clues to their function. Despite weak electron density, we successfully built these residues using the original data, now guided in part by the contiguous backbone density in the co-crystal structure¹⁴ (Figure 8; Figure S4A, Supporting Information). Along with the addition of the N-terminal residues, we successfully added several side chains that had been omitted from the H0 helix (Glu47, Glu49) resulting in an overall reduction in R_{free} and improved model geometry (Table S1, Supporting Information). The backbone density was reasonably well-defined for residues 33–38, while the side chain density varied. Significantly, Arg34 and Arg35 had the most well-defined side chains. The refined structure showed that Arg35 makes a potential salt bridge with Glu296 from Ins2 (Figure 8B; Figure S4B, Supporting Information) and Arg34 makes a potential salt bridge with Glu49 from the H0 α -helix while also making potential hydrogen bonding contacts with Asn46 (Figure 8C).

DISCUSSION

The peptide complementation assay developed here has allowed us to address several major questions not fully explained by previous biochemical or structural information. First, we have been able to address if both H0 insertions of the homodimer are required for splicing. Understanding the different roles of the two CYT-18 subunits in splicing has been challenging due to the difficulty of creating and purifying heterodimeric CYT-18. The CYT-18/Twort intron co-crystal structure established that H0 from one subunit was responsible for contacting the intron RNA directly, but the close proximity of H0 from the other subunit to the P5 region of the RNA,¹⁴ as well as site-directed hydroxyl cleavage data that placed H0 residues near P5¹³ suggested that both H0 insertions may be involved in splicing. By controlling the relative concentrations of the H0 peptide and CYT-18 protein, we demonstrated over a range of protein and peptide concentrations that ND1 splicing reaches a plateau when a maximum of 50% of the H0 binding site could be occupied. This strongly suggests that only a single H0 peptide is necessary for productive splicing. If the second H0 contacts the intron RNA, these interactions are not required for establishing a splicing-active intron conformation. It remains unclear why a drop in splicing activity was observed at equimolar concentrations of peptide to protein monomer at certain protein concentrations, though this may be related to concentration dependence observed in Figure 4. The drop in activity might imply negative cooperativity, though it is not clear why the activity would increase with the addition of more peptide. One possibility may be that the process of binding of the second peptide induces a local asymmetry in the protein dimer that negatively affects splicing. This subtle negative cooperativity could therefore be observed most prominently at or near conditions of peptide saturation. CYT-18 and bacterial

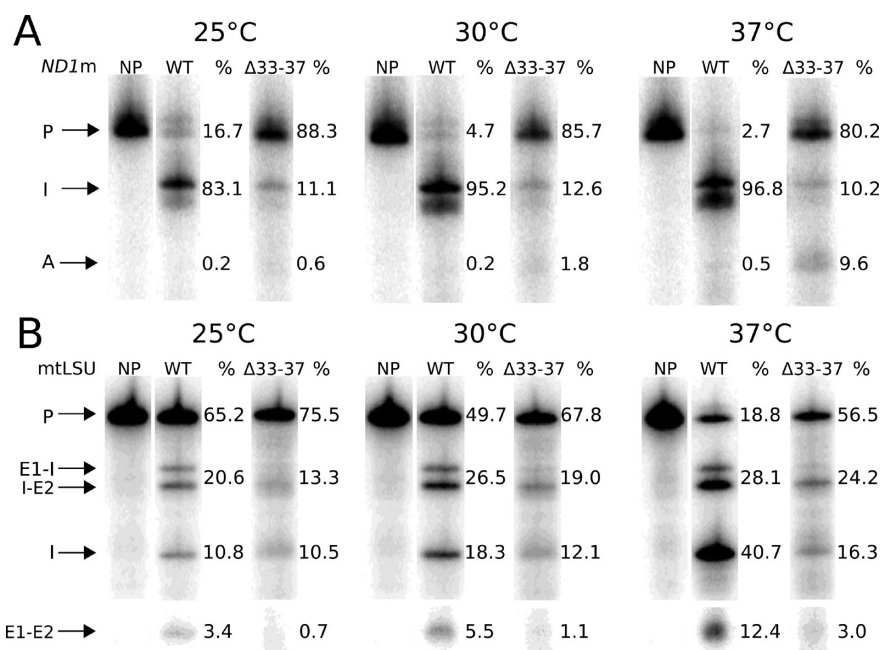


Figure 7. CYT-18/Δ33–37 group I intron splicing. Splicing was performed at 50 mM KCl at three temperatures for two *N. crassa* group I introns: (A) the ND1 intron and (B) the mt LSU intron. All products shown are following 60 min incubation at the given temperature. Products are labeled and quantified as in Figure 2.

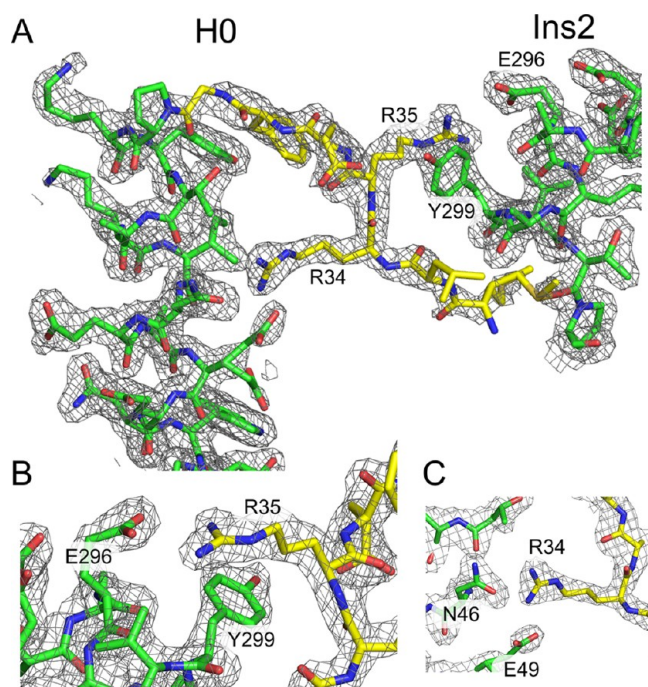


Figure 8. Structural evidence for ionic interactions by H0 N-terminal residues. (A) $2m|F_o| - D|F_c|$ electron density contoured at 1.0σ around H0 and Ins2 amino acids. H0 residues shown in yellow are newly built residues using the original CYT-18/Δ424–669 crystal structure data. (B) and (C) show the potential ionic interactions between Arg35 with Glu296 of Ins2, and Arg34 and Glu49 of H0, respectively.

TyrRSs all display half-of-sites reactivity in tRNA charging, which is thought to be an extreme case of negative cooperativity induced by dimer asymmetry.¹⁹

The peptide complementation assay has also provided the first evidence that the N-terminal most residues play an important role in intron splicing. On the basis of the CYT-18/Δ424–669

crystal structure, we reasoned that because a majority of the contacts between H0 and the rest of the CYT-18 protein were through hydrophobic interactions, H0 peptide truncations that retained those interactions would bind nearly as well as the H0-WT. Because only the N-terminus of H0's α -helical region was found to contact the Twort intron in the co-crystal structure, we anticipated that only peptides shortened beyond Pro39 would fail to complement splicing and that these peptides might function as competitive inhibitors of H0-WT complementation. The inability of the truncated peptides, including H0-37 which retained the entire α -helical sequence, to efficiently complement splicing or compete with H0-WT for complementation is consistent with the truncated peptides being unable to efficiently bind the protein at the H0 binding site, despite the peptides having all of the hydrophobic residues that make up a bulk of the interaction surface with the TyrRS core. Most simply, these results suggest that the five N-terminal residues that are present in H0-WT but absent in H0-37 must interact with either another part of the protein or the intron RNA to enhance peptide binding.

Splicing with the CYT-18/Δ33–37 protein showed significantly reduced splicing activity for both the ND1 and mt LSU introns, indicating that these first five residues are important for splicing in the context of the full-length protein and not just for peptide binding in the complementation assay. Further, CYT-18/Δ33–61 and CYT-18/Δ33–37 showed similar reduced mt LSU splicing activity in comparison to WT CYT-18 at all temperatures tested. Because CYT-18/Δ33–37 did not exhibit the same issues with solubility, the decreased mt LSU splicing activity for these and other N-terminal truncations is not likely due entirely to decreased protein stability as was previously ascribed.¹²

The peptide complementation assay has also provided initial evidence for how these residues may be functioning in the full-length protein. The H0-WT peptide showed a decreased ability to complement splicing at elevated monovalent salt and temperature. The CYT-18/group I intron interaction itself is salt-dependent,^{2,4,5} and the salt-dependence complementation could

simply reflect a decrease in intron affinity. However, previous studies indicated that binding and splicing were only reduced only at KCl concentrations greater than 100 mM at 37 °C.^{4,5} Because this is a tripartite system, the decrease in activity may also be due to decreased peptide affinity at higher salt and temperature, implicating ionic interactions.

Several other lines of analysis suggest that charged residues in the H0 N-terminus and Ins2 are being involved in ionic interactions. Most directly, we have been able to visualize this ionic interaction in the CYT-18/Δ424–669 crystal structure. We were able to build the missing N-terminal residues and show that Arg35 makes a potential salt bridge with Glu296 from Ins2. Previous biochemical data had implicated Glu296 and surrounding residues as being important in intron splicing. A short Ins2 deletion mutant that removed Glu296 inhibited ND1 intron splicing activity.¹³ The importance of this interaction is also evident from sequence analysis of *Pezizomycotina* mt TyrRSs.² Arg35 is highly conserved in the *Pezizomycotina* mt TyrRSs (15 of 18 species). One of these exceptions, *Stagansopora nodorum*, is believed to have lost its intron splicing activity, while another, *Podopspora anserina*, contains tandem lysine residues just N-terminal of the Arg34 position. Only the mt TyrRS from *Magnaporthe grisea* appears to lack basic residues at the H0 N-terminus. Previous sequence analysis revealed that Ins2 of *Pezizomycotina* mt TyrRSs lacked significant positional sequence conservation, but compositionally these insertions contained a large number of prolines and acidic residues.² Overall, these mt TyrRSs average four acidic residues in this 18 amino acid insertion, though notably the *M. grisea* mt TyrRS contains the fewest number of acidic residues with only two. The conserved charge distribution between the H0 N-terminus and Ins2 suggests an evolutionary conservation of ionic interactions between H0 and Ins2.

The CYT-18/group I intron complex has been a unique system for understanding how small protein adaptations can evolve to recognize distinct but related RNA substrates.^{2,13,20} Our study largely supports these previous results but hints at greater complexity. Previous structural information on CYT-18 showed that H0 makes side chain contacts with Ins1. This study establishes that H0 also interacts with Ins2, placing H0 in contact with both of the other N-terminal splicing insertions. It had been previously suggested that the role of H0 in splicing the mt LSU intron was primarily to stabilize another region of the protein that directly contacted the intron RNA.¹² This analysis can be explained by our results that suggest that the salt bridge between H0's N-terminal residues and Ins2 may be important for establishing the relative orientation of H0 and Ins2 during splicing. Thus, even if H0 does not directly contact some group I introns, it may still be important in helping to stabilize or position Ins1 and Ins2.

The development of a peptide complementation assay has allowed us to gain further insight into H0's role in group I intron splicing. Our results indicate that H0 serves as an important structural link that connects the N-terminal splicing insertions of CYT-18. It has been previously suggested that the highly specific structural features of the mt TyrRS splicing adaptations make them potentially unique targets for the development of antifungal drugs for *Pezizomycotina* species² such as *Histoplasma capsulatum*, *Coccidioides* sp., and *Aspergillus* sp. This study has elucidated a new role for H0's N-terminal residues, further highlighting it as a potentially targetable feature for drug development. Importantly, we have also demonstrated that an H0 peptide complementation can uncover important

features required for group I intron splicing activity. This assay will likely become a key tool in assessing small molecule inhibitors that could target mt TyrRS N-terminal insertions.

■ ASSOCIATED CONTENT

● Supporting Information

Figure S1, comparison of tyrosyl-adenylation assays for CYT-18, CYT-18/Δ33–61, and CYT-18/Δ33–37. Figure S2, peptide complementation for mt LSU intron splicing. Figure S3, circular dichroism spectra for the four peptides used in this study. Figure S4, structural views of the CYT-18/Twort cocrystal structure and the newly refined CYT-18/Δ442–669. Table S1, refinement statistics for re-refinement of the CYT-18/Δ442–669 structure. This material is available free of charge via the Internet at <http://pubs.acs.org>.

■ AUTHOR INFORMATION

Corresponding Author

*E-mail: paukstel@umd.edu; phone: 301-405-9933.

Funding

Funding was provided through University of Maryland startup funds.

Notes

The authors declare no competing financial interest.

■ ACKNOWLEDGMENTS

We thank Maithili Saoji and Daoning Zhang for technical assistance and Alan Lambowitz for comments on the manuscript.

■ ABBREVIATIONS

mt, mitochondrial; TyrRS, tyrosyl-tRNA synthetase; WT, wild-type; *N. crassa*, *Neurospora crassa*

■ REFERENCES

- (1) Akins, R. A., and Lambowitz, A. M. (1987) A protein required for splicing group I introns in *Neurospora* mitochondria is mitochondrial tyrosyl-tRNA synthetase or a derivative thereof. *Cell* 50, 331–345.
- (2) Paukstelis, P. J., and Lambowitz, A. M. (2008) Identification and evolution of fungal mitochondrial tyrosyl-tRNA synthetases with group I intron splicing activity. *Proc. Natl. Acad. Sci. U. S. A.* 105, 6010–6015.
- (3) Mohr, G., Zhang, A., Gianelos, J. A., Belfort, M., and Lambowitz, A. M. (1992) The *neurospora* CYT-18 protein suppresses defects in the phage T4 td intron by stabilizing the catalytically active structure of the intron core. *Cell* 69, 483–494.
- (4) Guo, Q., and Lambowitz, A. M. (1992) A tyrosyl-tRNA synthetase binds specifically to the group I intron catalytic core. *Genes Dev.* 6, 1357–1372.
- (5) Caprara, M. G., Mohr, G., and Lambowitz, A. M. (1996) A tyrosyl-tRNA synthetase protein induces tertiary folding of the group I intron catalytic core. *J. Mol. Biol.* 257, 512–531.
- (6) Caprara, M. G., Lehnert, V., Lambowitz, A. M., and Westhof, E. (1996) A tyrosyl-tRNA synthetase recognizes a conserved tRNA-like structural motif in the group I intron catalytic core. *Cell* 87, 1135–1145.
- (7) Myers, C. A., Wallweber, G. J., Rennard, R., Kemel, Y., Caprara, M. G., Mohr, G., and Lambowitz, A. M. (1996) A tyrosyl-tRNA synthetase suppresses structural defects in the two major helical domains of the group I intron catalytic core. *J. Mol. Biol.* 262, 87–104.
- (8) Chen, X., Mohr, G., and Lambowitz, A. M. (2004) The *Neurospora crassa* CYT-18 protein C-terminal RNA-binding domain helps stabilize interdomain tertiary interactions in group I introns. *RNA* 10, 634–644.

- (9) Vicens, Q., Paukstelis, P. J., Westhof, E., Lambowitz, A. M., and Cech, T. R. (2008) Toward predicting self-splicing and protein-facilitated splicing of group I introns. *RNA* 14, 2013–2029.
- (10) Chadee, A. B., Bhaskaran, H., and Russell, R. (2010) Protein roles in group I intron RNA folding: the tyrosyl-tRNA synthetase CYT-18 stabilizes the native state relative to a long-lived misfolded structure without compromising folding kinetics. *J. Mol. Biol.* 395, 656–670.
- (11) Cherniack, A. D., Garriga, G., Kittle, J. D., Akins, R. A., and Lambowitz, A. M. (1990) Function of *Neurospora* mitochondrial tyrosyl-tRNA synthetase in RNA splicing requires an idiosyncratic domain not found in other synthetases. *Cell* 62, 745–755.
- (12) Mohr, G., Rennard, R., Cherniack, A. D., Stryker, J., and Lambowitz, A. M. (2001) Function of the *Neurospora crassa* mitochondrial tyrosyl-tRNA synthetase in RNA splicing. Role of the idiosyncratic N-terminal extension and different modes of interaction with different group I introns. *J. Mol. Biol.* 307, 75–92.
- (13) Paukstelis, P. J., Coon, R., Madabusi, L., Nowakowski, J., Monzingo, A., Robertus, J., and Lambowitz, A. M. (2005) A tyrosyl-tRNA synthetase adapted to function in group I intron splicing by acquiring a new RNA binding surface. *Mol. Cell* 17, 417–428.
- (14) Paukstelis, P. J., Chen, J.-H., Chase, E., Lambowitz, A. M., and Golden, B. L. (2008) Structure of a tyrosyl-tRNA synthetase splicing factor bound to a group I intron RNA. *Nature* 451, 94–97.
- (15) Studier, F. W. (2005) Protein production by auto-induction in high density shaking cultures. *Protein Expr. Purif.* 41, 207–234.
- (16) Berman, H., Henrick, K., and Nakamura, H. (2003) Announcing the worldwide Protein Data Bank. *Nat. Struct. Biol.* 10, 980.
- (17) Emsley, P., Lohkamp, B., Scott, W. G., and Cowtan, K. (2010) Features and development of Coot. *Acta Crystallogr., Sect. D: Biol. Crystallogr.* 66, 486–501.
- (18) Murshudov, G. N., Vagin, A. A., and Dodson, E. J. (1997) Refinement of Macromolecular Structures by the Maximum-Likelihood Method. *Acta Crystallogr., Sect. D: Biol. Crystallogr.* 53, 240–255.
- (19) Ward, W. H., and Fersht, A. R. (1988) Asymmetry of tyrosyl-tRNA synthetase in solution. *Biochemistry* 27, 1041–1049.
- (20) Paukstelis, P. J., Chari, N., Lambowitz, A. M., and Hoffman, D. (2011) NMR structure of the C-terminal domain of a tyrosyl-tRNA synthetase that functions in group I intron splicing. *Biochemistry* 50, 3816–3826.